Energy Conversion and Management: X 20 (2023) 100424

Contents lists available at ScienceDirect

Energy Conversion and Management: X

journal homepage: www.sciencedirect.com/journal/energy-conversion-and-management-x

A combined analysis of the drying and decomposition kinetics of wood pyrolysis using non-isothermal thermogravimetric methods

Richard Ochieng [a,*], Alejandro L. Cerón [b], Alar Konist [b], Shiplu Sarker [a]

[a] Department of Civil and Manufacturing Engineering, Faculty of Engineering, Norwegian University of Science and Technology, NTNU, Teknologivegen 22, 2815 Gjøvik, Norway

[b] Department of Energy Technology, Tallin University of Technology, Ehitajate tee 5, 12616 Tallinn, Estonia

ARTICLE INFO

Keywords:
Wood
Thermogravimetric analysis
Drying
Thermal decomposition
Model-free methods
Error analysis

ABSTRACT

In this paper, we evaluate the pyrolysis of wood biomass as a combination of drying and thermal decomposition via the Page and modified Page models for drying kinetics as well as the Friedman and Vyazovkin methods for solid-state decomposition kinetics. This approach was applied to data obtained from thermogravimetric analysis of three wood species (spruce, pine, and birch) at 5, 20, and 30 K/min temperature programs.

According to the Page model, the average activation energies for spruce, pine, and birch wood between 30 and 150 °C were 12.87 ± 1.08, 13.32 ± 0.48, and 11.61 ± 0.59 kJ/mol, respectively. While all activation energies fell between 11.0 and 14.5 kJ/mol, the modified Page model predicted slightly higher energies, with an average absolute difference of 6.4% from Page's predictions. The activation energies and pre-exponential factors predicted by both models were lower at low heating rates, with the pre-exponential factor yielding significantly large differences between 5 and 30 K/min. These results showed that drying kinetics were significantly affected by heating rates. In addition, the goodness-of-fit analysis revealed that both models were reasonably accurate when predicting wood drying kinetics.

For the analysis of solid-state decomposition kinetics, a comparison of Friedman's linear differential method (FR) and Vyazovkin's nonlinear integral method (NLN-INT) was conducted at temperatures higher than 150 °C. In contrast to the NLN-INT method, the FR method predicted activation energies slightly higher, with an average absolute difference of about 8.4%. Evaluation of the relative errors revealed that both the FR and NLN-INT methods performed similarly. However, the Friedman (FR) method provided a reasonable fit to multistep decomposition kinetics through the simultaneous estimation of activation energies and pre-exponential factors. Nevertheless, the activation energies estimated by both the FR and NLN-INT methods were unreliable at conversions of $\alpha < 0.15$ and $\alpha > 0.85$. Validation of the kinetic results was conducted with differential thermogravimetric data at a heating rate of 5 K/min.

Introduction

In order to reduce net global carbon emissions by 2050, rapid deployment of biomass-based fuels to replace fossil fuels is necessary [1]. Technologies for converting lignocellulosic biomass, such as wood, mainly rely on thermochemical techniques like gasification, combustion, and pyrolysis to produce energy and biochemicals [2]. Pyrolysis, which is described as the thermal decomposition of biomass without any oxidizing agents, is the first and considered the most complex step in gasification and combustion technologies [3,4]. Wood pyrolysis usually starts with drying at temperatures lower than 200 °C, followed by the decomposition of lignocellulosic components such as hemicellulose, cellulose, lignin, and extractives [5]. Moisture in wood is present in three forms: as water vapor produced during solid decomposition; as hygroscopic water found in the cell wall, mainly hydrogen bonded to the hydroxyl groups of cellulose and hemicellulose, and to a lesser extent, lignin; and as free water found in liquid form in the void areas of biomass [6].

Previous studies have shown that thermogravimetric analysis (TGA) can deliver substantial details needed to understand the pyrolysis of lignocellulosic biomass at particle scale, while providing useful insights into the pyrolysis at reactor scale [7–9]. When applied on a reactor scale, the kinetic parameters derived from thermogravimetric analysis can be used accurately describe the gasification of biomass [10]. Moreover, when the sequential kinetic evaluation of biomass drying, and thermal

* Corresponding author.
E-mail address: richard.ochieng@ntnu.no (R. Ochieng).

https://doi.org/10.1016/j.ecmx.2023.100424
Received 14 March 2023; Received in revised form 10 July 2023; Accepted 11 July 2023
Available online 14 July 2023

Nomenclature

MR	Moisture ratio
M	Moisture content at temperature, T (%)
M_O	Initial moisture content (%)
M_e	Equilibrium moisture content (%)
$K-$	Drying coefficient (min^{-1})
K_O	Pre-exponential factor for drying (min^{-1})
T_O	Initial drying temperature (^oC)
T	Drying Temperature at any time (^oC)
$\beta-$	Heating rate $(K/\min)$
$t-$	Drying time (min.)
R	Universal gas constant $(JK^{-1}mol^{-1})$
E_d-	Activation energy of drying $(Jmol^{-1})$
N	Number of drying experiments at the different heating rates
NC	Number of drying parameters
χ^2	Reduced Chi-square
SSE	Standard error of estimate
α	degree of wood decomposition (conversion)
A	Pre-exponential factor for wood decomposition
m	weight of wood at time, t (%)
m_0	Initial weight of wood (%)
m_∞	Final weight of wood (%)
$I(E,T)$	Isoconverisonal temperature integral
FR	Friedman method
NLN-INT	Nonlinear integral method with numerical integration of $I(E,T)$
NLN-SY	Nonlinear integral method with the Senum -Yang's 4th -order approximation of $I(E,T)$
k	Number of thermal decomposition experiments at different heating rates
DTG	Differential thermogravimetric analysis
TG	Thermogravimetric analysis
E_α	activation Energy of wood decomposition at conversion, α
$E_{i,\alpha}$	activation Energy at conversion, α for $i = NLN-INT$, $NLN-SY$ or FR
r^2	Coefficient of determination for fitting the straight lines in Friedman plot
ε	Goodness of fit for nonlinear integral method (NLN-INT)

decomposition is undertaken at particle scale, the findings can reveal essential insights into the design of both the dryer and gasifier units needed for the pyrolysis at reactor scale [11,12].

Most researchers have assumed that the biomass used in TGA studies is almost dry after drying in an oven maintained at about 104 °C, thus water evaporation is either absent or very weak in the pyrolysis process [13]. However, other studies reveal that the sorption isotherms formed as result of the sorption of water vapor by biomass are multi-layered and temperature dependent, thus requiring higher energy levels to evaporate [14]. Furthermore, studies have also revealed that focusing only on solid-state decomposition kinetics during biomass pyrolysis can lead to unreliable estimation of activation energy values at low temperatures and conversions [15].

In the literature, a few studies have demonstrated that analyzing drying and thermal decomposition in sequence can provide useful insights into biomass pyrolysis. For instance; Chen et al.[16] investigated the kinetic analysis of raw corn straw and wheat straw using TGA with conversion ranges as $\alpha < 0.15$ for drying stage and $0.15-0.95$ for thermal decomposition. The authors observed consistently increasing values of activation energies for the combined drying and thermal decomposition of corn straw and wheat straw. Some crucial conclusions have also been revealed in the work published by Rueda-Ordóñez and Tannous [13] for the combined drying and thermal decomposition kinetics of sugarcane straw in inert and oxidative environments at heating rates of 2.5, 5 and 10 °C/min. In both studies, the subsequent stages of drying and thermal decomposition were set at 25 to 150 °C and 150 to 900 °C, respectively.

Among the drying models in the literature, the semi-theoretical models for biomass drying such as Page [17], Henderson and Pabis [18], Logarithmic [19], and modified Page [20] have been the most widely used to study the kinetics of biomass drying. These kind models present advantages over the theoretical and empirical models due their ease of use and ability to yield sufficiently reliable results on the drying behaviors of biomass [11,16,21].

In the literature, the Page model [20] has been considered the most reliable semi-theoretical model for predicting the drying kinetics of agricultural and forestry biomass [11,13,16].

Several thermogravimetric techniques for modeling the solid-state kinetics of biomass pyrolysis have been classified as "model-fitting" or "model-free" [22]. According to literature, most researchers prefer model-free methods, also known as isoconversional methods, due to their ability to produce relatively accurate predictions without requiring any model assumptions [23].

In the literature, numerous model-free methods have been used to study the kinetics of biomass pyrolysis. These include differential methods such as Friedman's (FR) [24] and integral methods such as Ozawa-Flynn-Wall (OFW) [25,26], Kissinger-Akahira-Sunose (KAS) [27,28], Starink [29], and Coats-Redfern [30]. In contrast to the Friedman method, which is derivative-based and requires no evaluation of the temperature integral, linear integral methods such as OFW, KAS, Starink, and Coats-Redfern require simplification of the temperature integral, resulting in substantial errors when estimating activation energies [31,32].

To overcome the limitations of linear integral methods, a non-linear integral method (NLN-INT) was proposed by Vyazovkin and co-authors in a series of publications [33–35]. The NLN-INT method is free of approximations and evaluates the temperature integral via numerical integration [34]. Some studies suggest that Senum and Yang's fourth-order approximation [34] can replace numerical integration in NLN-INT; however, its application is limited to a certain range of activation energy-to-temperature ratios, $x = E/RT$ [15,36]. As a result, numerical integration is likely the most effective way to estimate kinetic parameters with greater accuracy.

According to the literature, it has been reported that Friedman's (FR) or Vyazovkin's methods (NLN-INT) can lead to more accurate kinetic calculations than linear integral methods like OFW and KAS [32,37,38]. For instance; Sbirrazzuoli [23] used the isoconversional kinetic parameters derived from FR and NLN-INT methods to study reactions under different isothermal and nonisothermal conditions, and their accuracy was evaluated using data from simulated multi-step reactions. The findings reveal that both methods led to slight and similar error margins with simulated data. In another study, Budrugeac [39] evaluated the possibility of using the FR and NLN-INT to determine the activation energy (E), pre-exponential factor (A), and conversion function of a single-step process based on simulated non-isothermal data and experimental thermogravimetric data obtained from the thermo-oxidative degradation of polyvinyl chloride. The findings suggest that the FR or NLN-INT procedures can provide hints about the conversion function but cannot determine the actual expression definitively. Other studies comparing the performances of FR and NLN-INT methods based on simulated data and/or experimental data from non-biomass materials have also recently appeared in the literature [40,41].

Despite all the studies, most analyses have been conducted using either simulated data or experimental thermogravimetric data from non-biomass materials. As far as we are aware, there have not been many studies examining model-free methods involving biomass in comparison or analyzing their performance in depth. Additionally, previous studies have also demonstrated that the activation energies obtained by these methods at lower conversions could be unreliable [14]. Thus, coupled analysis of the drying and solid decomposition kinetics can be an effective approach in determining the activation energies over the entire degree of biomass conversions [13,16].

In this paper, we conduct comparative and in-depth error analyses of the Page and Modified Page models for modeling drying kinetics, as well as Friedman's (FR) and Vyazovkin's (NLN-INT) methods for modeling thermal decomposition kinetics of wood biomass. The models were deployed to examine the pyrolysis kinetics of three wood species (spruce, pine, and birch) based on the idea that pyrolysis is a combination of drying and solid-state decomposition. On the basis of these results, we can evaluate the application of TGA kinetic data to studies on a reactor scale.

Experimentation

Materials

Three wood samples, including two softwoods, Norway spruce (Picea abies) and Scots pine (Pinus sylvestris), and one hardwood, silver birch (Betula pendula), were pre-dried in an oven, crushed in a ball mill, and sieved in an Analysette 3 Pro Sieve to a particle size of < 250 μm, thus minimizing the mass and heat transfer effects during the experiments. Table 1 shows the proximate and ultimate compositions of wood species.

Thermogravimetric analysis

A thermogravimetric analyzer (Netzsch STA 449F3- Jupiter® – Thermal Analysis System, UK) was used to study the pyrolysis of wood samples at 5, 10, and 30 K/min over a temperature range of 30 to 950 °C. In each experiment, the end temperature was set at 1050 °C to account for the temperature difference between the sample and the reference (i.e., furnace) [42]. In each experiment, 5 mg ± 2 % of the sample was weighed and placed in Al_2O_3 crucibles without lids, and nitrogen at flow rate of 60 mL/min was used as a sweeping gas. After closing the TG with the sample inside, the system is purged for 30 min before starting the actual heating program. In order to reduce system errors, a correction was performed at each temperature program under identical experimental conditions. Each experiment was run at least twice to achieve a standard deviation of less than 1.0 %, and the average of the two subsequent data sets was considered.

Microsoft Excel, MATLAB® Software (version R2022a), and the Kinetic Calculation software proposed by Drozin et al.[15] were used for data analysis.

Table 1
Ultimate (dry basis) and proximate analysis (wet basis) of pine, spruce, and birch wood.

		Scots pine	Norway spruce	Silver birch
Proximate analysis (wt.%)	Moisture	8.5	6.9	7.7
	Volatile matter	85.2	85.5	86.9
	Fixed carbon	14.5	14.2	12.8
	Ash	0.3	0.3	0.3
Ultimate analysis (wt.%) (Dry basis)	C	50.1	50.3	49.3
	H	6.6	6.6	6.6
	N	0.19	0.1	0.08
	S	n.d.	n.d.	n.d.
	O*	43.1	42.7	44.0

n.d.– Not measured, * Calculated.

Theoretical part

Nonisothermal kinetic analysis of drying stage

The moisture ratio (MR) of biomass was calculated using the following equation [22].

$$MR = \left(\frac{M - M_e}{M_0 - M_e}\right) \tag{1}$$

Where M is the moisture content at temperature T, M_0 is the initial moisture content and M_e is the equilibrium moisture content at the conditions of the drying medium.

Since moisture-free carrier gas was used in this study, the values of M_e are relatively smaller than M and M_0, therefore can be ignored [11,16]. As a result, the dimensionless moisture ratio can be simplified as shown in equation (2):

$$MR = \frac{M}{M_0} \tag{2}$$

The expressions for the thin layer drying models of Page model [17], and modified Page [20] have been listed in Table 2.

where $t = \frac{T-T_0}{\beta}$,.$K = K_0 exp\left(-\frac{E_d}{R\,(T+273{,}15)}\right)$

$K$is the drying coefficient (min^{-1}), T_0 is the initial drying temperature (°C), T is the temperature at any time (°C), β is the heating rate (°C /min), and t is the drying time (min), K_0 is the pre-exponential factor (min^{-1}), R is the universal gas constant (J/mol/K), E_d is the activation energy of drying (J/mol), and a, b,and n are drying constants [16].

A nonlinear regression analysis using the particle swarm optimization algorithm [43] was implemented in MATLAB® Software (R2022a) to fit drying models to the experimental data.

In order to determine the goodness of fit, only the reduced chi-square $\chi 2$, and the residual standard error of estimate (SSE), as shown in equations (3) and (4), have been used in this study.

$$\chi^2 = \frac{\sum_{i=1}^{N}\left(\mathrm{MR}_{\mathrm{exp,i}} - \mathrm{MR}_{\mathrm{pred,i}}\right)^2}{\mathrm{N} - \mathrm{NC}} \tag{3}$$

$$SSE = \frac{\sum_{i=1}^{N}\left(MR_{expi} - MR_{predi}\right)^2}{N - NC}1/2 \tag{4}$$

where N is the number of experiments, and NC is the number of drying constants.

Lower values of the standard error estimate signify that the distances between the data points and the fitted values are smaller. Therefore, values of χ^2 and SSE which are the closest to zero, were considered for goodness of fit.

For the drying kinetics, the coefficient of determination has not been considered as a suitable goodness of fit for nonlinear regression, as this may be a statistically incorrect measure that often rarely shows any change before the third decimal point [44].

Additionally, previous studies have hardly obtained a coefficient of determination of less than 0.99 when using the Newton, Logarithmic, or Page drying models [11,16].

Kinetics analysis of solid-state decomposition

The reaction rate for a solid-state reaction is usually described by the equation (5) [22,45].

Table 2
Models for nonisothermal biomass drying.

Model	Model Equation	Reference
Page	$MR = exp[-Kt^n]$	[17]
Modified Page	$MR = exp[-(Kt)^n]$	[20]

$$\frac{d\alpha}{dt} = Aexp\left(-\frac{E}{RT}\right)f(\alpha) \tag{5}$$

where, A is the pre-exponential (frequency) factor, E is the activation energy, T is the absolute temperature, R is the gas constant, $f(\alpha)$ is the reaction model, and α is the conversion fraction.

For gravimetric measurements, the conversion α, which is also known as normalized mass $\alpha \in [0,1]$ is defined in equation (6) below;

$$\alpha = \left(\frac{m_0 - m_t}{m_0 - m_\infty}\right) \tag{6}$$

where, m_0 is initial weight, m_t is weight at time t, and m_∞ is the final weight.

For nonisothermal rate expression, equation (5) can be transformed by replacing the isothermal reaction rate,(dα/dt) with a reaction rate function of temperature, $(d\alpha/dT)$ and a constant heating rate, $\beta = dT/dt$. The differential form of the nonisothermal rate law then becomes,

$$\frac{d\alpha}{dT} = \frac{A}{\beta}exp\left(-\frac{E}{RT}\right)f(\alpha) \tag{7}$$

The solution of equation (7) takes an integral form of nonisothermal rate law as;

$$g(\alpha) = \int_0^\alpha \frac{d\alpha}{f(\alpha)} = \frac{A}{\beta}\int_{T_0}^{T} e^{-(E/RT)}dT = \frac{A}{\beta}I(E,T) \tag{8}$$

where, $g(\alpha)$ is the integral reaction model and $I(E,T)$ is the temperature integral that has no analytical solution, but can be approximated using numerous functions [32].

The possible reaction models of $f(\alpha)$ and $g(\alpha)$ are classified according to their mechanistic basis as nucleation, geometrical contraction, diffusion, and reaction order as shown in Table 3.

For integral methods, the oversimplified approximations of the temperature integral in equation (8) can induce large errors in the estimated activation energy values [33,34]. However, the application of the Senum and Yang's fourth-order approximation [46] of the temperature integral has been reported to reduce these errors [36]. The Senum-Yang's fourth order approximation of $I(E,T)$ is expressed as in equation (9);

Table 3
Reaction models and their integral forms used in *iso*-conversional methods [22].

Model	Differential form,$f(\alpha)$	Integral form, g (α)
	Nucleation models	
Power law (P2)	$2\alpha^{1/2}$	$\alpha^{1/2}$
Power law (P3)	$3\alpha^{2/3}$	$\alpha^{1/3}$
Power law (P4)	$4\alpha^{3/4}$	$\alpha^{1/4}$
Avrami-Erofeyev (A2)	$2(1-\alpha)[-\ln(1-\alpha)]^{1/2}$	$[-\ln(1-\alpha)]^{1/2}$
Avrami-Erofeyev (A3)	$3(1-\alpha)[-\ln(1-\alpha)]^{2/3}$	$[-\ln(1-\alpha)]^{1/3}$
Avrami-Erofeyev (A4)	$4(1-\alpha)[-\ln(1-\alpha)]^{3/4}$	$[-\ln(1-\alpha)]^{1/4}$
	Diffusion models	
1-D diffusion(D1)	$1/(2\alpha)$	α^2
2-D diffusion(D2)	$-[1/\ln(1-\alpha)]$	$[(1-\alpha)\ln(1-\alpha)]+\alpha$
3-D diffusion-Jander (D3)	$\left[3(1-\alpha)^{2/3}\right]/\left[2\left(1-(1-\alpha)^{1/3}\right)\right]$	$\left[1-(1-\alpha)^{1/3}\right]^2$
Ginstling-Brounshtein (D4)	$\left[3(1-\alpha)^{1/3}\right]/\left[2\left(1-(1-\alpha)^{1/3}\right)\right]$	$1-(2/3)\alpha-(1-\alpha)^{2/3}$
	Reaction models	
Zero-order (F0/R1)	1	α
First-order (F1)	$(1-\alpha)$	$-\ln(1-\alpha)$
Second-order (F2)	$(1-\alpha)^2$	$[1/(1-\alpha)]-1$
Third-order (F3)	$(1-\alpha)^3$	$(1/2)\left[(1-\alpha)^{-2}-1\right]$

$$I(E,T) \approx \frac{exp(-x)}{x}\pi(x) \tag{9}$$

where $x = E/(RT)$ and.$\pi(x) = \frac{x^3+18x^2+88x+96}{x^4+20x^3+120x^2+240x+120}$

The Friedman and the nonlinear method (NLN-INT) methods require no approximation of the temperature integral, $I(E,T)$.

Friedman method

The Friedman's method is derived by rearranging equation (7) to obtain equation (10) below;

$$\ln\left[\beta_i\left(\frac{d\alpha}{dT}\right)_{\alpha,i}\right] = \ln[A_\alpha f(\alpha)] - \frac{E_\alpha}{RT_{\alpha,i}} \tag{10}$$

where the subscript i means i^{th} heating rate. The E_α values at given α, can be estimated by using multiple heating rates, β_i without any known $f(\alpha)$ or $g(\alpha)$.

In the linear fittings of $\ln\left[\beta_i(d\alpha/dT)_{\alpha,i}\right]$ vs. $-1/T_{\alpha,i}$, E_α can be estimated from the slope E_α/R; and the corresponding pre-exponential factor, A_α can be calculated from the intercepts once the most suitable $f(\alpha)$ is known.

Nonlinear isoconversional method

The integral nonlinear method (NLN-INT) proposed by Vyazovkin [34] is free of approximations and makes use of numerical integration to solve the temperature integral. Just like all the other integral isoconversional methods, this method assumes that the reaction model,$g(\alpha)$ is independent of the heating program, β.

For a set of K experiments conducted at different heating programs β_i, the activation energy values can be determined at any conversion value, α by finding the value of E_α that minimizes the function, $\phi(E_\alpha)$ as described in equation (11);

$$\phi(E_\alpha) = \sum_{i=1}^{k}\sum_{j\neq i}^{k}\frac{\left[I\left(E_\alpha, T_{\alpha,i}\right)\beta_j\right]}{\left[I\left(E_\alpha, T_{\alpha,j}\right)\beta_i\right]} \tag{11}$$

where

$$I(E_\alpha, T_\alpha) = \int_{T_{\alpha-\Delta\alpha}}^{T_\alpha} \exp\left(\frac{-E_\alpha}{RT}\right)dT \tag{12}$$

The subscripts i and j represent ordinal numbers of two experiments performed under different heating programs. Although literature shows that sophisticated algorithms such as genetic algorithm can be applied to find the minimum [47], the curve$\phi(E_\alpha)$has a parabolic form and a unique minimum (see; support information); therefore, even a simple unconstrained optimization method can be used to find the minimum [15]. The integral (equation (11) with the limits $T_{\alpha-\Delta\alpha}$ and T_α is evaluated numerically over a small increment Δα that allows to eliminate the accumulation of systematic errors in E_α calculation. The conversion α is varied from Δα to 1-Δα with a step $\Delta\alpha = 1/X$, where X is the number of intervals chosen for analysis [34].

In this study, the calculation procedure was implemented in a Microsoft Excel macro [48], which was earlier developed for the work presented by Joseph et al. [49], and 100 intervals were chosen. The macro uses the trapezoidal rule and a uniform grid spacing, that is continually decreased until a difference in the integral values smaller than 10^{-6} between consecutive iterations is obtained.

The Kinetic Calculation software developed by Drozin et al. [15] was used to determine the kinetic parameters of wood decomposition based on Vyazovkin's method that uses the Senum-Yang's 4th order approximation for the temperature integral (NLN-SY). With the tool, one of the advantages is that it improves accuracy by considering the actual heating rate via the least square error minimization of the temperature program. To make a comparison, the results obtained by Vyazovkin's method, which uses the trapezoidal rule (NLN-INT), were compared

with those obtained by the NLN-SY.

Results and discussion

Thermogravimetric analyses

The TG [(1 − α) vs. T] and DTG [− dm/dt vs.T] profiles for the pyrolysis of spruce, pine, and birch wood at heating rates of 5 K/min, 10 K/min, and 30 K/min are displayed in Figs. S1, S2 and S3 of the supplementary information. The pyrolysis process was divided into the drying stage (Stage I) and the thermal decomposition stage (Stage II). At the initial temperatures of 30 to ~ 110 °C, mass loss of approximately 5 to 7 % occurred in Stage I as the moisture content rapidly decreased due to significant evaporation. As the wood was continuously heated, it was likely that the rapid diffusion of water vapor led to the need for moisture evaporation [50]. The moisture loss increased up to a temperature of 120 °C before flattening off, as indicated by the TG and DTG curves. Previous studies have shown that weight loss due to moisture between ambient and 150 °C can be as much as 10% [51].

This study assumed the drying process was complete once the temperature reached 150 °C, ensuring all moisture had evaporated. Several other authors have also considered this temperature in their studies [13,16,50,52]. As shown in Fig. 1, the mass loss curves reveal that pine, spruce, and birch wood decomposed most rapidly in the temperature ranges of 243–370 °C, 231–370 °C and 243–370 °C, respectively, at 5 K/min. Perhaps the rapid conversion was due to the complex chemical reactions that take place at these temperature ranges [53].

When the heating rate was increased to 30 K/min, the upper limit shifted towards higher temperatures. These temperatures would be 415 °C, 406 °C, and 410 °C for spruce, pine, and birch wood, respectively. The results were consistent with previous studies that observed rapid decomposition of wood dust between 250 and 450 °C [54].

From the mass loss vs temperature plots, the main peak in the DTG curves was due to cellulose decomposition, while the shoulder at lower temperatures can be attributed to the pyrolysis of hemicellulose [14,55]. Compared to hardwood decomposition, softwood decomposition starts at lower temperatures, and has a delayed hemicellulose shoulder, as shown in Fig. 1. Birch wood contains more hemicellulose than the softwood species (pine and spruce), causing the "hemicellulose" decomposition shoulder to be more visible [55]. For all the wood samples, a flattening line became apparent with increasing temperature, indicating slow lignin degradation [5,51].

Additionally, the double (10 K/min) and sixfold (30 K/min) increases in the heating rates from 5 K/min shifted the maximum temperature of the DTG curve by 12 and 35 °C for spruce, 17 and 42 °C for pine, and 13 and 39 °C for birch, respectively. The shifts can be attributed to heat and mass transfer limitations caused by the shorter residence time needed for wood to reach a higher temperature [51]. The observations agreed with the temperature differences reported by the International Confederation for Thermal Analysis and Calorimetry (ICTAC) [42,45]. The reader may refer to Figs. S1, S2 and S3 in the supplementary information for more details.

Analysis of drying kinetics

The Page and modified Page models were used to study the drying kinetics of wood at heating rates of 5 and 30 K/min. The fitting parameter values were estimated using an unconstrained particle swarm optimization algorithm [43].

All the models provided good agreement between the experimental and theoretical moisture ratio, *MR* as indicated by the statistical values of the Standard error of estimate, SSE, and the chi-square value, χ^2 which was also the objective function. All the wood samples (spruce, pine, and birch) and heating rates (5 and 30 K/min), the χ^2 and SSE values remained below $1x10^{-4}$ and 0.007 respectively for both the Page and modified Page Models, as shown in Table 4. The significantly low values of the statistical parameters, χ^2 and SSE indicated good fits for both the Page and modified Page model.

As shown in Table 4, the Page and modified Page models predicted consistent values of the activation energies, E_d and pre-exponential factors,K_0. Additionally, both models showed an increasing trend in activation energies with heating rates for spruce, pine, and birch wood. These findings were consistent with previous studies reported by Chen et. al. [16].

Using Page's model, the average values of activation energy for drying spruce, pine, and birch wood were 12.87 ± 1.08, 13.32 ± 0.48, and 11.61 ± 0.59 kJ/mol, respectively. There was a possibility that pine's high moisture content contributes to its high drying activation energies at all heating rates. Generally, the activation energies and pre-exponential factors for all wood species increased at higher heating rates. While the activation energies only varied from 11.0 to 14.5 kJ/mol for both the Page and modified Page models, the pre-exponential factors significantly increased (over 450%) between 5 and 30 K/min. Based on these results, it was concluded that the heating rate has a significantly greater effect on the pre-exponential factors than the activation energies of wood drying.

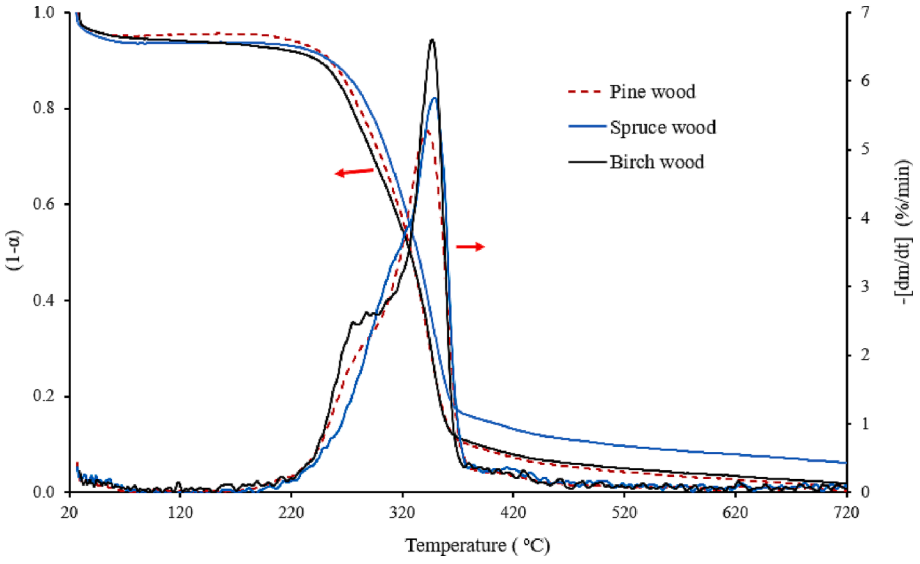

Fig. 1. TG $(1-\alpha)$ and DTG $[-dm/dt]$ curves for spruce, pine, and birch wood at 10 K/min.

Table 4
Estimated drying kinetic parameters for spruce, pine, and birch wood at 5 and 30 K/min.

Biomass	Model	β	K_0/min	E(kJ/mol)	n	$\chi^2 x\ 10^{-5}$	SSE
		5	13.80	11.6624	0.9694	0.81424	0.00286
Spruce wood	Page	30	81.76	14.0858	0.9597	3.9477	0.00628
	modified Page	5	14.99	12.0300	0.96942	8.1424	0.00286
		30	76.59	13.9456	0.97891	4.3651	0.00661
		5	17.46	12.7000	0.97160	2.1452	0.00463
Pine wood	Page	30	57.30	13.9385	0.9734	2.1452	0.00463
	modified Page	5	18.98	13.0817	0.97160	2.4766	0.00498
		30	53.73	13.7827	0.989707	1.5246	0.00390
		5	19.19	11.3300	0.90136	1.1714	0.00342
Birch wood	Page	30	53.23	11.8868	0.8974	3.1421	0.00561
	modified Page	5	26.51	11.4600	0.90136	1.7319	0.00342
		30	83.85	13.2457	0.89740	3.1422	0.00561

The modified Page model predicted slightly higher energies, with an average absolute difference of 6.4% from Page's predictions. The values of the kinetic parameter n varied in the range 0.9 to 1.0 for all the models and wood samples. As a result of the low standard error estimates and chi-square values, both models were found to be reasonably accurate in predicting the kinetics of wood drying. Fig. 2 illustrates the fit of the Page model to experimental data for spruce, pine, and birch wood samples at 30 K/min. The results of this study were consistent with those of previous studies using other biomass types [16,50,56].

According to the literature, parameters for biomass drying under an inert atmosphere ranged from 1 to 50 kJ/mol for activation energies and 0.9 to 1.7 for n [11,13,50,57]. In the supplemented document, additional information, such as residual errors and correlations between experimental and estimated moisture ratios, was provided.

Analysis of thermal decomposition kinetics

In the thermal decomposition stage, the FR and NLN-INT methods were used to determine the dependencies of activation energies on conversion for temperatures above 150 °C i.e., α = 0.1–0.95. To estimate the exact TGA and DTG data points for the desired conversions, Langrage's three-point interpolation method was applied.

The analysis results from the FR method for spruce, pine and birch wood were presented in the $\ln[\beta_i(d\alpha/dt)_\alpha]$ vs. $-1/T_\alpha$ plots shown in Figs. S13–S15 of the supplementary information. The $\ln[\beta_i(d\alpha/dt)_\alpha]$ vs. $-1/T_\alpha$ plots yielded straight lines, and the apparent activation energies, E_α were estimated from the slopes at each conversion, ranging from $\alpha =$ 0.1 to 0.95 with a step size of 0.05. The mean apparent activation energies predicted by FR method in the conversion range of $\alpha = 0.1$ and 0.8 for pine, spruce, and birch wood were 157.63 ± 5.67, 157.33 ± 12.11 and 160.69 ± 9.57 kJ/mol, respectively. These results were consistent with previous studies in the literature [53,58,59].

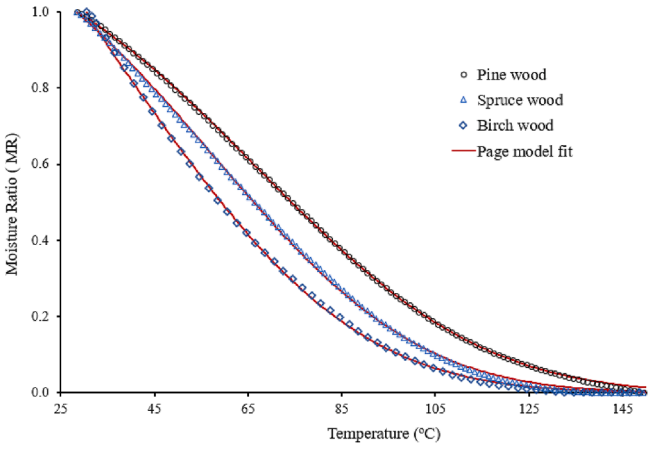

Fig. 2. Experimental and predicted (Page model) moisture ratios for pine, spruce, and birch wood at 30 K/min.

According to the r^2 vs. α plot in Fig. 3, the straight-line plots presented a good fit until a conversion of $\alpha = 0.85$, at which point the r^2 values suddenly dropped to values as low as 0.5 for all wood species. Previous studies have also reported similar trends in the literature [58]. The low values of r^2 indicate the limitations of the Friedman method in predicting accurate values of apparent activation energies at higher conversions [42].

For non-linear integral method (NLN-INT), ref.[38] suggested that the accuracy in E_α evaluation can be measured by $\varepsilon = 1 - \left|\phi(E_\alpha)_{\min} - k(k-1)\right| / k(k-1)$, where $\phi(E_\alpha)_{\min}$ was the minimum value of $\phi(E_\alpha)$ associated with the non-linear procedure in equation (11), and k is the number of heating programs. The values of ε close to unity indicated accurate values of E_α.

According to Fig. 4, values of ε were greater than 0.99 for all the wood species in the conversion range of $0.1 \leqslant \alpha \leqslant 0.8$. Just like the r^2 in the FR method, the ε values for the NLN-INT approach significantly decreased to lower values, indicating inaccuracies in the predicted values of E_α at conversions higher than 0.8.

While the high activation energy can be attributed to the slow decomposition of lignin at higher conversions [51], the low values of r2 and ε indicated that the associated values of Eα might not be accurate. The low values of r2 at higher conversion rates were consistent with previous studies [16,58].

When the difference between the maximum and minimum values of E_α is less than 10 % of the average E_α, E_α is independent of α, and the process occurs through a single-step mechanism [60]. However, in this study, the difference between maximum and minimum values of E_α was above 16.7 % and 29.1% of the average E_a for FR and NLN-INT methods, respectively. Therefore, the pyrolysis of wood biomass followed a multi-step reaction mechanism [6]. In that case, the isoconversional principle was used to approximate the process kinetics by considering multiple single-step kinetic equations, each of which could be associated with a specific activation energy, E_α or conversion, α [42].

The E_α vs. α plots for the FR, NLN-INT, and NLN-SY methods are shown in Figs. 5(a–c) for spruce, pine, and birch wood, respectively. The inherent characteristics of the lignocellulosic components in the wood influenced the variations in activation energy values at the various conversion stages [61]. The early increase in the apparent activation can be attributed to the decomposition of hemicellulose in the conversion range of 0.1–0.4. Beyond α = 0.45, the downward trend may be attributed to the decomposition of cellulose which was characterized by a decrease in activation energies with conversion [58]. In contrast to hemicellulose and lignin, the activation energies for the decomposition of cellulose essentially remained unchanged with conversion [61]. Above α = 0.65, the activation energy values increased, and later sharply increased at conversions of over 0.85. The increased in activation energy values was attributed to the decomposition of lignin which occurs slowly over a wider temperature range [61]. The observed variations in the activation energy values resulted from the use of a simple

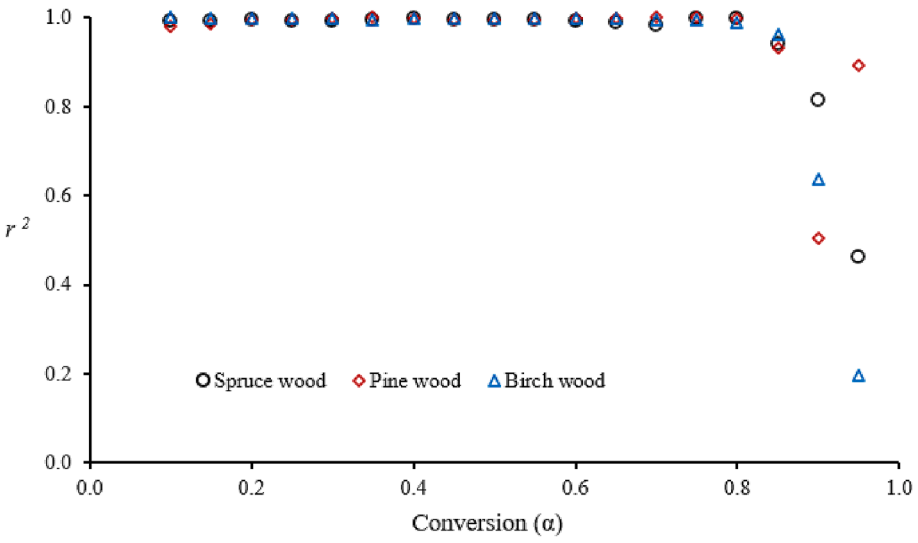

Fig. 3. Fit for FR method (r^2) with conversion (α) for spruce, pine, and birch wood.

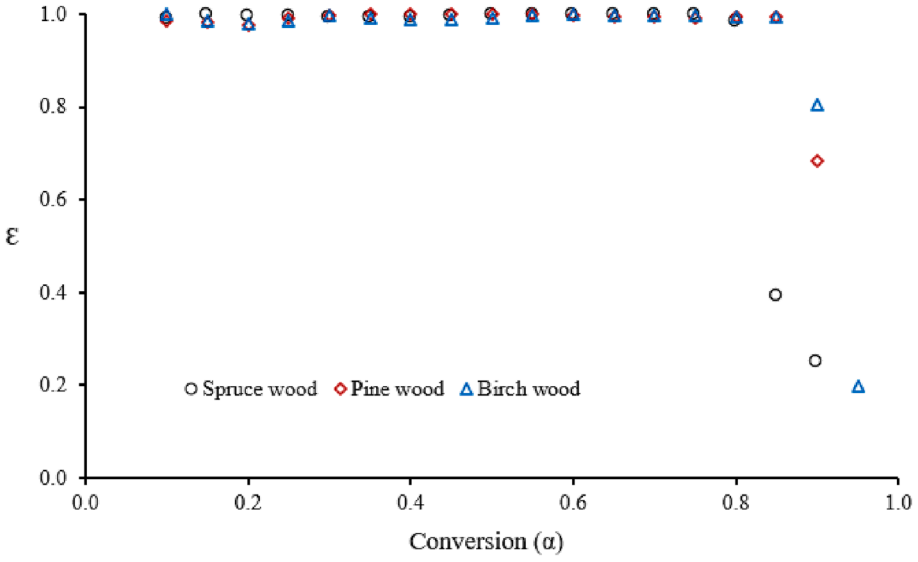

Fig. 4. Fit for NLN-INT method (ε)with conversion (α) for spruce, pine, and birch wood.

differential form in the FR method and various techniques for calculating temperature integrals in integral methods [51].

In general, the *FR* method predicted slightly higher values of activation energies than the NLN-INT and NLN-SY methods. According to the literature, these findings appeared to be true for decomposition reactions involving an increase in E_α values with α [37]. Furthermore, while the FR method predicted higher activation energy values at low ($\alpha < 0.15$) and high ($\alpha > 0.85$) conversion levels, the NLN-INT method indicated the reverse. Even though neither result was reliable, it was possible that the variations at low and high conversion were due to different derivation strategies applied by the two methods [37,38].

As shown in Fig. 6, further comparison of FR and NLN-INT revealed that the average difference ($|E_{FR,\alpha} - E_{NLN-INT,\alpha}|$) between $E_{FR,\alpha}$ and $E_{NLN-INT,\alpha}$ in the conversion range $\alpha = 0.15 - 0.8$ were within ± 10.9 kJ/mol for all the wood species. In this range, the difference between $E_{FR,\alpha}$ and $E_{NLN-INT,\alpha}$ decreased with *e* in conversion. The observation agreed with previous studies in the literature [37].

The average absolute relative deviation of $E_{FR,\alpha}$ with respect to $E_{NLN-INT,\alpha}$ was ≈ 8.4 %. This error indicated a close match in performance of the FR and NLN-INT methods, and similar findings have also been reported in the literature [23,37,38].

In Fig. 7, a comparison of relative errors in activation energies between Vyazovkin's numerical integration method (NLN-INT) and that involving temperature integral approximation (NLN-SY) is presented. Within the conversion range of 0.2 and 0.8, all wood species had relative activation energy errors between 2.0 and 8.0 percent. As a result, approximating the temperature integral in NLN-INT might help simplify iterative calculations in situations where small errors are acceptable.

Determination of the kinetic model and pre-exponential factors

The Kinetic Calculation Software assumes a Sestak and Berggren reaction model [62], $f(\alpha) = \alpha^w(1-\alpha)^z[-\ln(1-\alpha)]^p$, and through a definition of the pre-exponential factor *A*, a model-fitting method to minimize the error between the predicted and experimental DTG curves was applied to determine the parameters w, z, p and A. More details on the procedure can be found in Drozin et al. [15].

The findings of the analyses of spruce, pine, and birch woods are reported in Table 5.

Even though the values of the pre-exponential factor, A obtained

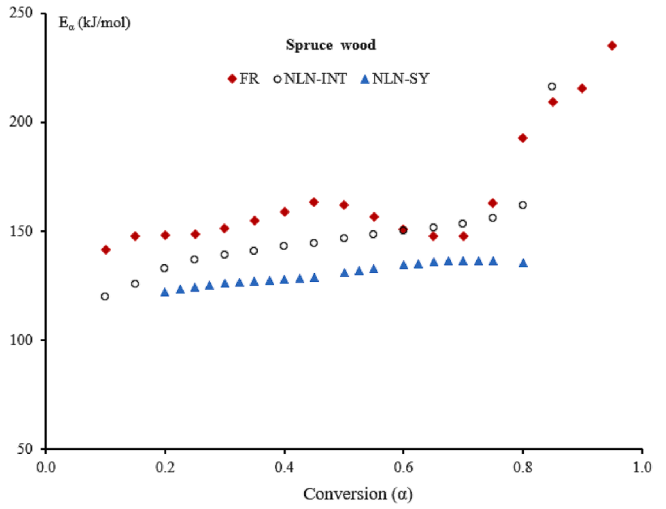

Fig. 5a. Dependence of activation energies (E_α) on conversion (α) for spruce wood.

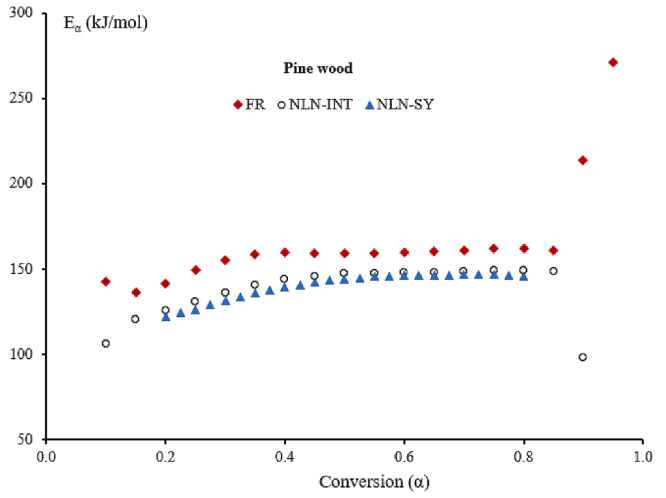

Fig. 5b. Dependence of activation energies (E_α) on conversion (α) for pine wood.

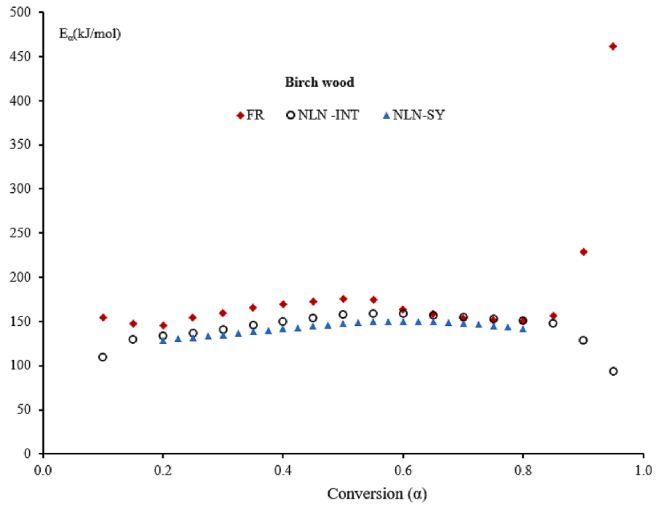

Fig. 5c. Dependence of activation energies (E_α) on conversion (α) for birch wood.

from the Software were within range with the average results obtained in the literature [58], the dependency of $\ln A_\alpha$ vs. α cannot be predicted from the program. Using a linear model fitting method, the software yields a single value for the preexponential factor, A. Consequently, the kinetic calculation software cannot be used to generate multiple single-step reactions in order to approximate multi-step reaction mechanisms in wood biomass [42]. To predict the variation of A_α with α, nonlinear fitting models will need to be applied simultaneously to the DTG data retrieved at different heating rates [63].

To determine the $\ln A_\alpha$ vs. α, the generalized master plot approach proposed by the ref.[64] was applied to the results obtained from the Friedman method. The most suitable reaction mechanism, $f(\alpha)$ for the pyrolysis of the wood samples was one that gave the best match between the experimental and theoretical values of λ(α), as described in Equation (13). The latter was determined by evaluating the possible reaction models in Table 3. In this work, only the accelerating models, such as the reaction order and diffusional models that described processes whose concentrations decreased with conversion, have been considered for evaluation [42].

$$\lambda(\alpha) = \frac{f(\alpha)}{f(\alpha)_{0.5}} = \frac{(d\alpha/dt)_\alpha}{(d\alpha/dt)_{0.5}} \frac{\exp[E/(RT_\alpha)]}{\exp[E_{0.5}/(RT_{0.5})]} \tag{13}$$

where $T_{0.5}$, $(d\alpha/dt)_{0.5}$and$E_{0.5}$ are the temperature, DTG and apparent activation energy values at $\alpha = 0.5$.

The effective value of activation energy, E was determined by applying the minimizing procedure proposed by Hu et al.[58], as described in Equation (14).

$$E = min \sum \left(\frac{E - E_\alpha}{E}\right) x100 \tag{14}$$

According to Fig. 8, the diffusional model (D3) was selected as a single rate-limiting step kinetic representation that closely estimates the multi-step reaction processes for all the wood species.

The kinetic compensation effect for pre-exponential factors, A_α and activation energies, E_α were used to demonstrate the validity of the determined reaction mechanism [65,66]. The existence of the compensation effect suggested that all $\ln A_\alpha$ and E_α pairs were linearly correlated as $\ln A_\alpha = q^* E_\alpha + b$, where q and b are constants. Even though the $\ln A_\alpha$ and E_α values significantly varied with conversion α; the correlation fitted well into straight lines as shown in the constable plots in Fig. 9. The goodness of fit, u^2 for spruce, pine and birch wood were 0.993, 0.995 and 0.986, respectively.

Figs. 10(a–c) show a comparison of the experimental data and theoretically determined DTG curves $(d\alpha/dT)$ for spruce, pine, and birch woods, respectively. In all cases, the FR method matched the experimental data closely, including predictions of peak DTG and shoulder values. The findings agreed with those predicted in the previous studies [51]. It was possible to attribute the shape of the FR prediction to the compensation effect between variations in activation energy and frequency factors [39,55]. It is possible that the discrepancy between the experimental result and the NLN-SY prediction has been caused by systematic errors in using a single value for A.

Conclusions

In this study, we have shown that thin-layer drying models can be sequentially combined with model-free methods to predict water evaporation and solid-state decomposition during the pyrolysis of wood biomass (spruce, pine, and birch).

By applying a global optimization algorithm for nonlinear regression analysis, both the Page and modified Page models predicted distinct and consistent activation energies and pre-exponential factors without any need for initial guesses. The average activation energies for drying spruce, pine, and birch wood were estimated to be 12.87 ± 1.08, 13.32 ± 0.48, and 11.61 ± 0.59 kJ/mol, respectively. However, this would

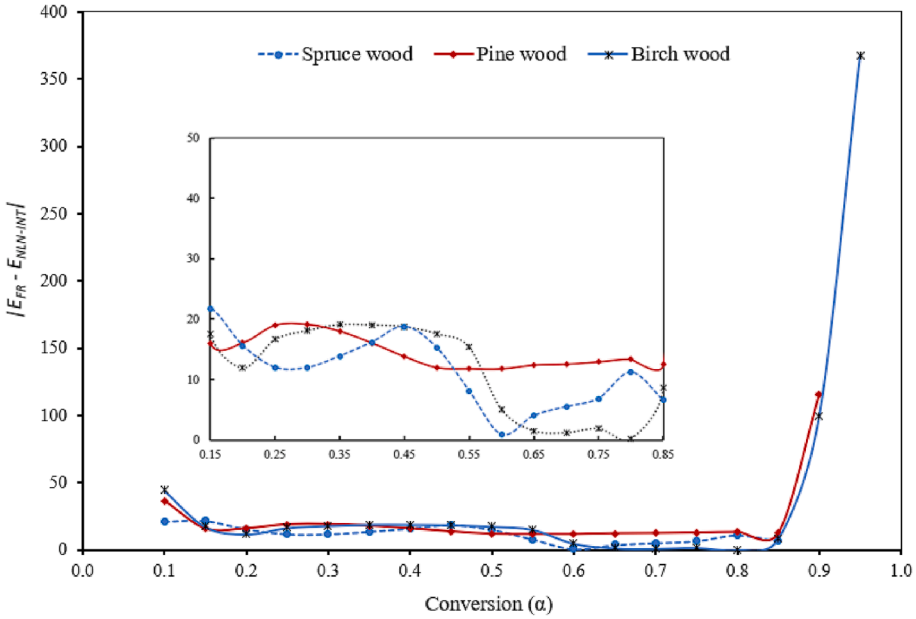

Fig. 6. Activation energy differences, $\left|E_{FR,\alpha} - E_{NLN-INT,\alpha}\right|$ with conversion (α) for spruce, pine, and birch.

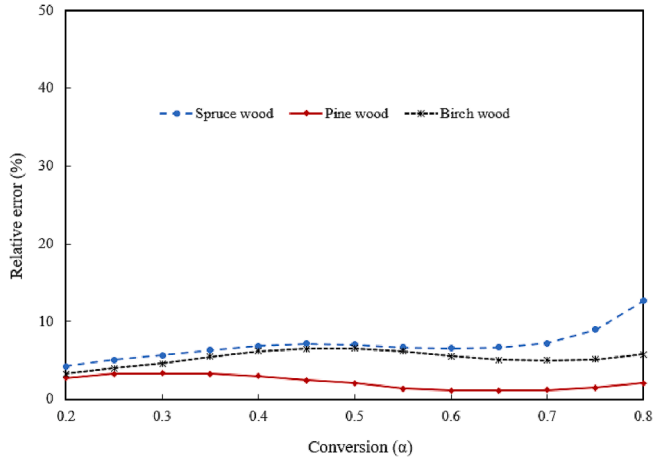

Fig. 7. Dependence of relative errors $\left|E_{NLN-SY,\alpha} - E_{NLN-INT,\alpha}\right|$ x100/$E_{NLN-INT,\alpha}$ on conversion (α) for spruce, pine, and birch wood.

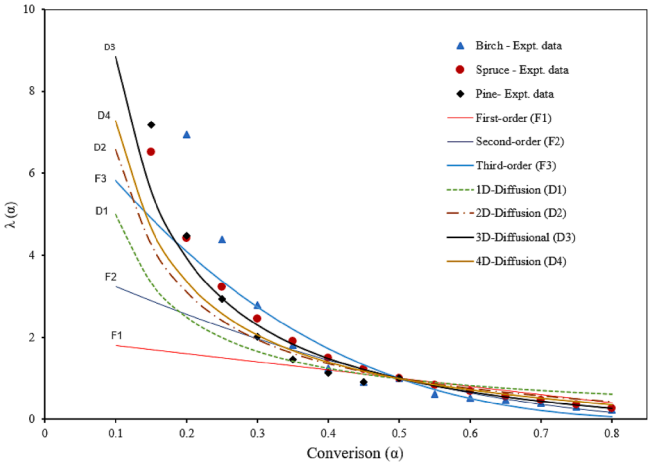

Fig. 8. Theoretical and experimental $\lambda(\alpha)$ master-plots of the possible reaction mechanisms for spruce, pine, and birch wood.

Table 5
Kinetic triplets from the NLN-SY method.

Wood	Pre-exponential factor, A	w	z	p
Spruce	3.53×10^{10}	0.1	1.81	0
Pine	4.46×10^{11}	0.7	1.99	0
Birch	5.465×10^{11}	0.1	1.99	0

likely vary with the moisture content of the biomass. Furthermore, heating rates appear to affect drying kinetics more through pre-exponential factors than activation energies.

For thermal decomposition, the main mass loss for both softwoods (pine and spruce) and hardwoods occurred between 220 and 420 °C. In contrast to hardwoods, the thermal decomposition of softwoods started at lower temperatures and exhibited a delayed hemicellulose shoulder at heating rates of 5, 20, and 30 K/min.

For all the wood species, activation energies estimated by Friedman (FR) and nonlinear integral (NLN-INT) methods were both reliable and remarkably similar, in the conversion range of 0.15 – 0.8. Error analyses revealed that activation energies estimated by the Vyazovkin or Friedman methods were unreliable at conversion levels above 0.85.

In contrast to the Vyazovkin (NLN-INT), the Friedman (FR) method provided a reliable estimate of the multi-step decomposition of the wood by calculating both activation energies and pre-exponential factors when the reaction mechanism was known. The software recently proposed by Drozin, and co-authors offers a quick estimation of the kinetic triplets; however, further improvements are needed to include the variation of the pre-exponential factor with conversion. Future applications of thermogravimetric data to pyrolysis reactor modeling can benefit from model-free methods such as Friedman's, which can predict both activation energies and pre-exponential factors for each biomass component in the multi-step kinetic mechanism.

CRediT authorship contribution statement

Richard Ochieng: Conceptualization, Writing – original draft. **Alejandro L. Cerón:** Methodology, Writing – review & editing, Data curation. **Alar Konist:** Resources, Writing – review & editing, Supervision. **Shiplu Sarker:** Writing – review & editing, Supervision, Project

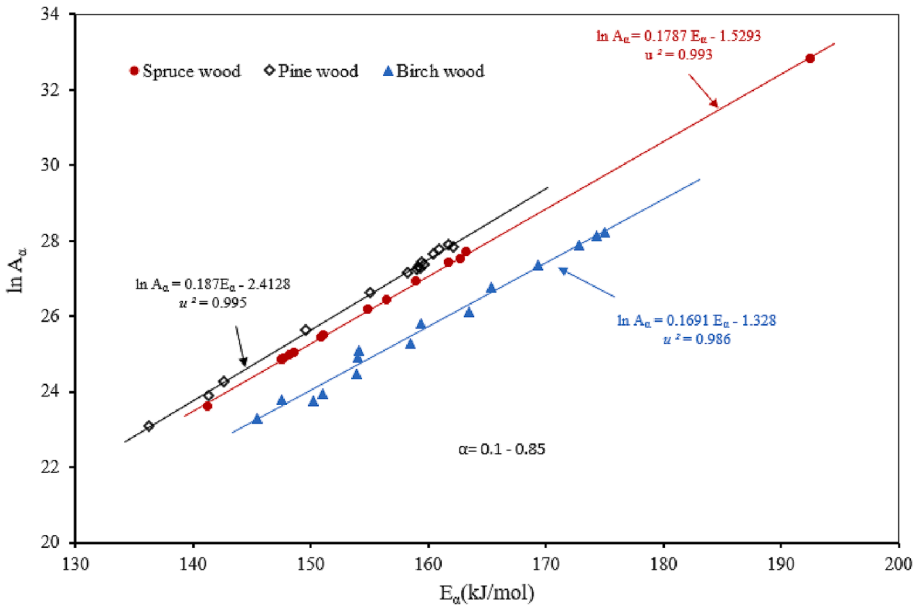

Fig. 9. The compensation effects for the pyrolysis of spruce, pine, and birch wood.

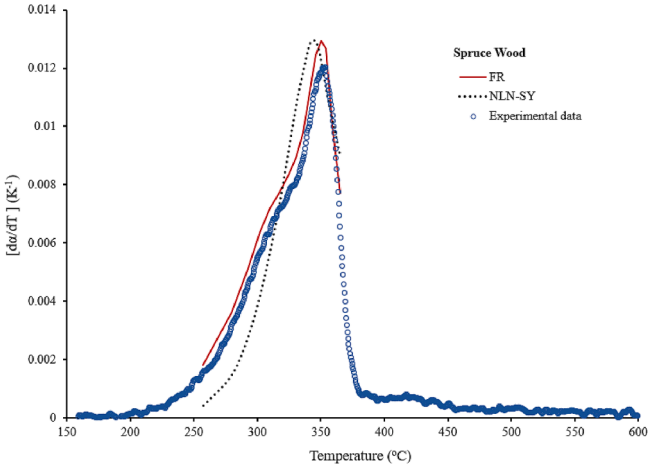

Fig. 10a. Experimental and calculated curves $d\alpha/dT$ for spruce wood at β = 5 K/min.

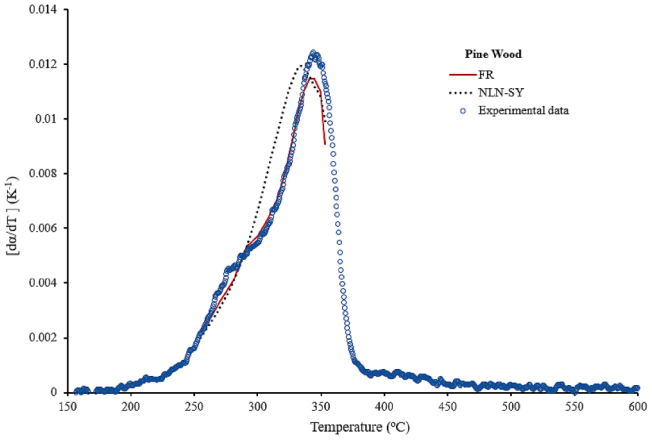

Fig. 10b. Experimental and calculated curves $d\alpha/dT$ for pine wood at β = 5 K/min.

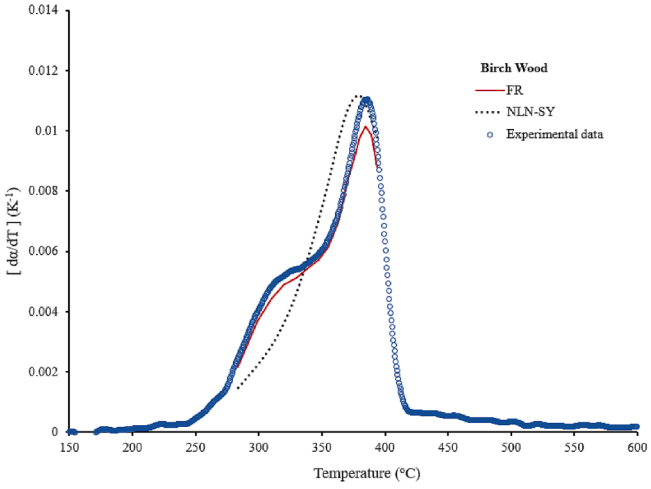

Fig. 10c. Experimental and calculated curves $d\alpha/dT$ for birch wood at β = 5 K/min.

administration.

Declaration of Competing Interest

The authors declare the following financial interests/personal relationships which may be considered as potential competing interests: Shiplu Sarker reports financial support was provided by Nordic Energy Research.

Data availability

Data will be made available on request.

Acknowledgements

The authors would like to acknowledge the Nordic Energy Research for providing financial support via the BIOELEC project, grant no. 120006. Furthermore, we would like to acknowledge Prof. Alemayehu Gebremedhin for undertaking a thorough review and providing valuable

remarks on the manuscript.

Appendix A. Supplementary data

Supplementary data to this article can be found online at https://doi.org/10.1016/j.ecmx.2023.100424.

References

[1] IEA. Bioenergy. IEA. Lisense: CC BY 4.0, Paris 2022. https://www.iea.org/reports/bioenergy (accessed January 22, 2023).
[2] Saravanakumar A, Vijayakumar P, Hoang AT, Kwon EE, Chen W-H. Thermochemical conversion of large-size woody biomass for carbon neutrality: Principles, applications, and issues. Bioresour Technol 2023;370:128562.
[3] Di Blasi C. Modeling chemical and physical processes of wood and biomass pyrolysis. Prog Energy Combust Sci 2008;34(1):47–90.
[4] Hoang AT, Ong HC, Fattah IMR, Chong CT, Cheng CK, Sakthivel R, et al. Progress on the lignocellulosic biomass pyrolysis for biofuel production toward environmental sustainability. Fuel Process Technol 2021;223:106997.
[5] Demirbas A, Arin G. An overview of biomass pyrolysis. Energy Source 2002;24(5):471–82.
[6] Anca-Couce A. Reaction mechanisms and multi-scale modelling of lignocellulosic biomass pyrolysis. Prog Energy Combust Sci 2016;53:41–79.
[7] Di Blasi C. Combustion and gasification rates of lignocellulosic chars. Prog Energy Combust Sci 2009;35(2):121–40.
[8] Sharma A, Pareek V, Zhang D. Biomass pyrolysis—A review of modelling, process parameters and catalytic studies. Renew Sustain Energy Rev 2015;50:1081–96.
[9] Luo H, Wang X, Liu X, Wu X, Shi X, Xiong Q. A review on CFD simulation of biomass pyrolysis in fluidized bed reactors with emphasis on particle-scale models. J Anal Appl Pyrol 2022;162:105433.
[10] Felix CB, Chen W-H, Ubando AT, Park Y-K, Lin K-Y, Pugazhendhi A, et al. A comprehensive review of thermogravimetric analysis in lignocellulosic and algal biomass gasification. Chem Eng J 2022;445:136730.
[11] Cai J, Chen S. Determination of Drying Kinetics for Biomass by Thermogravimetric Analysis under Nonisothermal Condition. Drying Technol 2008;26(12):1464–8.
[12] Wang S, Dai G, Yang H, Luo Z. Lignocellulosic biomass pyrolysis mechanism: A state-of-the-art review. Prog Energy Combust Sci 2017;62:33–86.
[13] Rueda-Ordóñez YJ, Tannous K. Drying and thermal decomposition kinetics of sugarcane straw by nonisothermal thermogravimetric analysis. Bioresour Technol 2018;264:131–9.
[14] Grønli MG, Várhegyi G, Di Blasi C. Thermogravimetric Analysis and Devolatilization Kinetics of Wood. Ind Eng Chem Res 2002;41(17):4201–8.
[15] Drozin D, Sozykin S, Ivanova N, Olenchikova T, Krupnova T, Krupina N, et al. Kinetic calculation: Software tool for determining the kinetic parameters of the thermal decomposition process using the Vyazovkin Method. SoftwareX 2020;11:100359.
[16] Chen D, Zheng Y, Zhu X. In-depth investigation on the pyrolysis kinetics of raw biomass. Part I: Kinetic analysis for the drying and devolatilization stages. Bioresour Technol 2013;131:40–6.
[17] Page GE. Factors Influencing the Maximum Rates of Air Drying Shelled corn in Thin Layers., Agricultural engineering. Purdue University, West Lafayette, Indiana., Purdue e-Pubs; 1949.
[18] Hendorson SM. Grain Drying Theory (I) Temperature Effect on Drying Coefficient. J Agric Eng Res 1961;6:169–74.
[19] Akgun NA, Doymaz I. Modelling of olive cake thin-layer drying process. J Food Eng 2005;68(4):455–61.
[20] Overhults DG, White GM, Hamilton HE, Ross IJ. Drying soybeans with heated air. Transactions of the ASAE.1973; 16 (1): 112.
[21] Mühlbauer W, Müller J. Chapter 2.1 - Drying kinetics. In: Mühlbauer W, Müller J, editors. Drying Atlas. Woodhead Publishing; 2020. p. 53–61.
[22] Khawam A, Flanagan DR. Solid-State Kinetic Models: Basics and Mathematical Fundamentals. J Phys Chem B 2006;110(35):17315–28.
[23] Sbirrazzuoli N. Model-free isothermal and nonisothermal predictions using advanced isoconversional methods. Thermochim Acta 2021;697:178855.
[24] Friedman HL. Kinetics of thermal degradation of char-forming plastics from thermogravimetry. Application to a phenolic plastic. J Polym Sci, Part C: Polym Symp 1964;6(1):183–95.
[25] Flynn JH, Wall LA. A quick, direct method for the determination of activation energy from thermogravimetric data. J Polym Sci, Part B: Polym Lett 1966;4(5):323–8.
[26] Ozawa T. A New Method of Analyzing Thermogravimetric Data Bulletin of the Chemical Society of Japan 1965; 38 (11): 1881-1886.
[27] Kissinger HE. Reaction Kinetics in Differential Thermal Analysis. Anal Chem 1957;29(11):1702–6.
[28] Akahira T, Sunose TT. Joint Convention of Four Electrical Institutes, Report of Research. Chiba Institute of Technology; 1971. p. 22–31.
[29] Starink MJ. The determination of activation energy from linear heating rate experiments: a comparison of the accuracy of isoconversion methods. Thermochim Acta 2003;404(1):163–76.
[30] Coats AW, Redfern JP. Kinetic Parameters from Thermogravimetric Data. Nature 1964;201(4914):68–9.
[31] Sbirrazzuoli N. Is the Friedman Method Applicable to Transformations with Temperature Dependent Reaction Heat? Macromol Chem Phys 2007;208(14):1592–7.
[32] Sbirrazzuoli N, Vincent L, Mija A, Guigo N. Integral, differential and advanced isoconversional methods: Complex mechanisms and isothermal predicted conversion–time curves. Chemom Intel Lab Syst 2009;96(2):219–26.
[33] Vyazovkin S. Evaluation of activation energy of thermally stimulated solid-state reactions under arbitrary variation of temperature. J Comput Chem 1997;18(3):393–402.
[34] Vyazovkin S. Modification of the integral isoconversional method to account for variation in the activation energy. J Comput Chem 2001;22(2):178–83.
[35] Vyazovkin S. A unified approach to kinetic processing of nonisothermal data. Int J Chem Kinet 1996;28(2):95–101.
[36] Vyazovkin S, Dollimore D. Linear and Nonlinear Procedures in Isoconversional Computations of the Activation Energy of Nonisothermal Reactions in Solids. J Chem Inf Comput Sci 1996;36(1):42–5.
[37] Budrugeac P, Segal E. On the nonlinear isoconversional procedures to evaluate the activation energy of nonisothermal reactions in solids. Int J Chem Kinet 2004;36(2):87–93.
[38] Budrugeac P. Differential Non-Linear Isoconversional Procedure for Evaluating the Activation Energy of Non-Isothermal Reactions. J Therm Anal Calorim 2002;68(1):131–9.
[39] Budrugeac P. On the use of the model-free way method for kinetic analysis of thermoanalytical data – advantages and limitations. Thermochim Acta 2021;706:179063.
[40] Li K, Gan C, Zhang W, Li C, Li G. Validity of isothermal kinetic prediction by advanced isoconversional method. Chem Phys 2023;567:111801.
[41] Granado L, Sbirrazzuoli N. Isoconversional computations for nonisothermal kinetic predictions. Thermochim Acta 2021;697:178859.
[42] Vyazovkin S, Burnham AK, Criado JM, Pérez-Maqueda LA, Popescu C, Sbirrazzuoli N. ICTAC Kinetics Committee recommendations for performing kinetic computations on thermal analysis data. Thermochim Acta 2011;520(1):1–19.
[43] Wang D, Tan D, Liu L. Particle swarm optimization algorithm: an overview. Soft Comput 2018;22(2):387–408.
[44] Spiess A-N, Neumeyer N. An evaluation of R2 as an inadequate measure for nonlinear models in pharmacological and biochemical research: a Monte Carlo approach. BMC Pharmacol 2010;10(1):6.
[45] Vyazovkin S, Chrissafis K, Di Lorenzo ML, Koga N, Pijolat M, Roduit B, et al. ICTAC Kinetics Committee recommendations for collecting experimental thermal analysis data for kinetic computations. Thermochim Acta 2014;590:1–23.
[46] Senum GI, Yang RT. Rational approximations of the integral of the Arrhenius function. Journal of thermal analysis.1977;;11(3):445–7.
[47] Mohajeri S, Vafayan M, Ghanbaralizadeh R, Pazokifard S, Zohuriaan Mehr MJ. Advanced isoconversional cure kinetic analysis of epoxy/poly(furfuryl alcohol) bio-resin system. J Appl Polym Sci 2017;134(42):45432.
[48] Bernardes CES. MS Excel Worksheet for Isoconversional Activation Energy Calculations by Vyazovkin's Method, https://webpages.ciencias.ulisboa.pt/~cebernardes/Software-macros.html (downloaded october 20 2022).
[49] Joseph A, Bernardes CES, Druzhinina AI, Varushchenko RM, Nguyen TY, Emmerling F, et al. Polymorphic Phase Transition in 4′-Hydroxyacetophenone: Equilibrium Temperature, Kinetic Barrier, and the Relative Stability of $Z' = 1$ and $Z' = 2$ Forms. Cryst Growth Des 2017;17(4):1918–32.
[50] Chen D-Y, Zhang D, Zhu X-F. Heat/mass transfer characteristics and nonisothermal drying kinetics at the first stage of biomass pyrolysis. J Therm Anal Calorim 2012;109(2):847–54.
[51] Mishra G, Kumar J, Bhaskar T. Kinetic studies on the pyrolysis of pinewood. Bioresour Technol 2015;182:282–8.
[52] Cai JM, Bi LS. Kinetic analysis of wheat straw pyrolysis using isoconversional methods. J Therm Anal Calorim 2009;98(1):325–30.
[53] Chen Z, Hu M, Zhu X, Guo D, Liu S, Hu Z, et al. Characteristics and kinetic study on pyrolysis of five lignocellulosic biomass via thermogravimetric analysis. Bioresour Technol 2015;192:441–50.
[54] Koullas DP, Nikolaou N, Koukios EG. Modelling non-isothermal kinetics of biomass prepyrolysis at low pressure. Bioresour Technol 1998;63(3):261–6.
[55] Grønli M. Theoretical and experimental study of the thermal degradation of biomass. In: Dept of Thermal Energy and Hydropower. The Norwegian University of Science and Technology; 1996. p. 282.
[56] Chen D, Zheng Y, Zhu X. Determination of effective moisture diffusivity and drying kinetics for poplar sawdust by thermogravimetric analysis under isothermal condition. Bioresour Technol 2012;107:451–5.
[57] Fernandez A, Saffe A, Mazza G, Rodriguez R. Nonisothermal drying kinetics of biomass fuels by thermogravimetric analysis under oxidative and inert atmosphere. Drying Technol 2017;35(2):163–72.
[58] Hu M, Chen Z, Wang S, Guo D, Ma C, Zhou Y, et al. Thermogravimetric kinetics of lignocellulosic biomass slow pyrolysis using distributed activation energy model, Fraser-Suzuki deconvolution, and iso-conversional method. Energ Conver Manage 2016;118:1–11.
[59] Soria-Verdugo A, Goos E, García-Hernando N. Effect of the number of TGA curves employed on the biomass pyrolysis kinetics results obtained using the Distributed Activation Energy Model. Fuel Process Technol 2015;134:360–71.
[60] Pouretedal HR, Ravanbod M. Kinetic study of ignition of Mg/NaNO3 pyrotechnic using non-isothermal TG/DSC technique. J Therm Anal Calorim 2015;119(3):2281–8.
[61] Wang S, Lin H, Ru B, Dai G, Wang X, Xiao G, et al. Kinetic modeling of biomass components pyrolysis using a sequential and coupling method. Fuel 2016;185:763–71.

[62] Šesták J, Berggren G. Study of the kinetics of the mechanism of solid-state reactions at increasing temperatures. Thermochim Acta 1971;3(1):1–12.
[63] Brown ME, Maciejewski M, Vyazovkin S, Nomen R, Sempere J, Burnham A, et al. Computational aspects of kinetic analysis: Part A: The ICTAC kinetics project-data, methods and results. Thermochim Acta 2000;355(1-2):125–43.
[64] Sánchez-Jiménez PE, Pérez-Maqueda LA, Perejón A, Criado JM. Generalized master plots as a straightforward approach for determining the kinetic model: The case of cellulose pyrolysis. Thermochim Acta 2013;552:54–9.
[65] Ding J, Zhang X, Hu D, Ye S, Jiang J. Model-free kinetic determination of pre-exponential factor and reaction mechanism in accelerating rate calorimetry. Thermochim Acta 2021;702:178983.
[66] Vyazovkin S. Determining Preexponential Factor in Model-Free Kinetic Methods: How and Why? Molecules 2021;26(11):3077.